

Rapid long-range proton diffusion along the surface of the purple membrane and delayed proton transfer into the bulk

(pH indicator dye/fluorescein/bioenergetics/chemiosmotic coupling)

U. ALEXIEV*, R. MOLLAAGHABABA†, P. SCHERRER*, H. G. KHORANA†, AND M. P. HEYN*

*Biophysics Group, Department of Physics, Freie Universität, Berlin, Arnimallee 14, D-14195, Berlin, Germany; and †Departments of Biology and Chemistry, Massachusetts Institute of Technology, 77 Massachusetts Avenue, Cambridge, MA 02139

Contributed by H. G. Khorana, September 9, 1994

ABSTRACT The pH-indicator dye fluorescein was covalently bound to the surface of the purple membrane at position 72 on the extracellular side of bacteriorhodopsin and at positions 101, 105, 160, or 231 on the cytoplasmic side by reacting bromomethylfluorescein with the sulfhydryl groups of cysteines introduced by site-directed mutagenesis. At position 72, on the extracellular surface, the light-induced proton release was detected $71 \pm 4 \mu\text{s}$ after the flash (conditions: pH 7.3, 22°C, and 150 mM KCl). On the cytoplasmic side with the dye at positions 101, 105, and 160, the corresponding values were 77, 76, and $74 \pm 5 \mu\text{s}$, respectively. Under the same conditions, the proton release time in the bulk medium as detected by pyranine was around 880 μs —i.e., slower by a factor of more than 10. The fact that the proton that is released on the extracellular side is detected much faster on the cytoplasmic surface than in the aqueous bulk phase demonstrates that it is retained on the surface and migrates along the purple membrane to the other side. These findings have interesting implications for bioenergetics and support models of local proton coupling. From the small difference between the proton detection times by labels on opposite sides of the membrane, we estimate that at 22°C the proton surface diffusion constant is greater than $3 \times 10^{-5} \text{ cm}^2/\text{s}$. At 5°C, the proton release detection time at position 72 equals the faster of the two main rise times of the M intermediate (deprotonation of the Schiff base). At higher temperatures this correlation is gradually lost, but the curved Arrhenius plot for the proton release time is tangential to the linear Arrhenius plot for the rise of M at low temperatures. These observations are compatible with kinetic coupling between Schiff base deprotonation and proton release.

Models of localized energy coupling by proton gradients require a transient confinement of protons near the membrane, allowing lateral proton transport along the surface between proton sources and sinks (1). Thus, protons must be retained at the surface long enough for significant lateral diffusion to occur. This requires that the rate of proton transfer into the bulk is slow compared with the rate of transport along the surface (2, 3). To determine these rates, dynamic methods of sufficient time resolution are required (4). The purple membrane of *Halobacterium salinarium* offers an ideal model system to study these questions. The purple membrane patches of about 0.5- μm diameter contain approximately 10^4 light-driven proton pumps. Using a nanosecond light flash these proton pumps are simultaneously activated, and protons are released on the extracellular side of the membrane about 50–100 μs after excitation. Thus, a transient jump in proton concentration is generated along the extracellular side of the membrane, which dissipates by diffusion along the membrane and by transfer into the bulk phase. Proton arrival times at

different sites on either side of the membrane can be measured spectroscopically with surface-bound pH-indicator dyes and compared with the detection time in the bulk phase using the water-soluble dye pyranine. To attach a dye at any desired position on the surface, we introduced a single cysteine residue by site-directed mutagenesis, and its sulfhydryl group was used to covalently bind the proton indicator dye fluorescein. In previous work we have used this method to measure the proton release time on either side of bacteriorhodopsin (bR) (5–7) and to determine the surface charge density in bR micelles from the salt dependence of the apparent pK of the bound dye (8). These studies showed that protons released on the extracellular side of bR were detected faster at the cytoplasmic side of the protein than in the bulk phase (5, 6). Moreover, when the proton mobility along the micellar surface was varied by using lipids with head groups of different pK values and proton dwell times, the proton signal at the cytoplasmic side changed in a predictable way (5, 6). These experiments provided evidence that the protons are initially retained at the surface and migrate faster along the micellar surface to the other side of bR than they transfer into the bulk. We now confirm and extend these results with purple membranes. Their much larger size permits lateral proton migration over longer distances and may allow an estimate of the proton diffusion constant. Our results confirm that there is a rapid proton equilibration along both sides of the purple membrane and a 10-fold delayed appearance of protons in the bulk phase. The proton detection times on the two sides of the membrane are almost the same. This allows the calculation of a lower bound of $3 \times 10^{-5} \text{ cm}^2/\text{s}$ for the proton diffusion constant along the membrane, which is only one-third that in bulk water. Further, a comparison of the kinetics of the rise of the M intermediate (deprotonation of the Schiff base) and the kinetics of proton release as detected at the extracellular surface has allowed an insight into the mechanism of proton transport within bR. Possible coupling between the above two reactions was investigated by measuring the temperature dependence of their rate constants.

MATERIALS AND METHODS

Tris was obtained from Sigma. EDTA and 1,4-dithio-DL-threitol were from Fluka. Sephadex G-25 (fine) was from Pharmacia, and 5-(bromomethyl)fluorescein (BMF) was from Molecular Probes.

The preparation of the bR mutants G72C, V101C, and Q105C, in which cysteine is substituted for Gly-72, Val-101, and Gln-105, respectively, has been reported (9). The bR mutants A160C and G231C, in which cysteine replaces Ala-160

Abbreviations: bR, bacteriorhodopsin; G72C, V101C, Q105C, A160C, or G231C bR mutant containing a substitution of cysteine for Gly-72, Val-101, Gln-105, Ala-160, or Gly-231, respectively; G72C-MF, V101C-MF, Q105C-MF, A160C-MF, or G231C-MF, methylfluorescein derivative of the G72C, V101C, Q105C, A160C, or G231C mutant; BMF, 5-(bromomethyl)fluorescein.

The publication costs of this article were defrayed in part by page charge payment. This article must therefore be hereby marked "advertisement" in accordance with 18 U.S.C. §1734 solely to indicate this fact.

and Gly-231, respectively, were prepared by following the described procedures (10) except that the synthetic restriction fragments *Bsp*HI-*Psp*1406I and *Sph*I-*Not*I were used respectively for construction of the mutant genes.

bR (0.1 μ mol) and BMF (1 μ mol) were allowed to react in 1 ml of 50 mM Tris buffer, pH 7.0/150 mM KCl/4 μ M EDTA/0.1 mM dithiothreitol under argon at room temperature. After 90 min the excess reagents were removed by chromatography on Sephadex G-25, preequilibrated, and eluted with Milli-Q system (Millipore)-purified water. The labeling stoichiometry, fluorescein per bR, was determined spectroscopically by using an extinction coefficient of $\epsilon = 68,000 \text{ M}^{-1}\cdot\text{cm}^{-1}$ (Molecular Probes) for the alkaline form of fluorescein at 495 nm and of $\epsilon = 63,000 \text{ M}^{-1}\cdot\text{cm}^{-1}$ for bR at 570 nm. The apparent pK_a of methylfluorescein bound to position 72 (G72C-MF) was 7.0 in 150 mM KCl.

Flash spectroscopy and data analysis with a sum of exponentials were performed as described elsewhere (11). The excitation was with 10-ns pulses of 3–6 mJ of energy at 590 nm. Under these conditions 15% of the bR molecules were found to photocycle. Typically 30–50 signals were averaged for the kinetics of M and 70–100 for the dye kinetics.

Proton release and uptake were detected in the aqueous bulk medium of the purple membrane suspension, containing 4–15 μ M bR in 150 mM KCl, by measuring the difference of the flash-induced absorbance changes at 450 nm (12) between samples with and without 45 μ M pyranine (8-hydroxy-1,3,6-pyrenetrisulfonic acid trisodium salt; Serva) at pH 7.3 and 22°C. The light-induced proton concentration changes detected with fluorescein attached to cysteine residues in bR were determined by measuring the flash-induced absorbance difference at 495 nm (13) between samples with and without 10 mM Tris buffer at pH 7.3 and 22°C and in 150 mM KCl.

RESULTS

Labeling with BMF. Methylfluorescein was covalently bound to cysteine residues introduced by site-directed mutagenesis at Gly-72 (BC loop) on the extracellular side and at Val-101 (CD loop), Gln-105 (CD loop), Ala-160 (EF loop), and Gly-231 (carboxyl-terminal tail) on the cytoplasmic side of

bR (Fig. 1), generating G72C-MF, V101C-MF, Q105C-MF, A160C-MF, and G231C-MF mutants, respectively. These residues were selected because their replacement by cysteine causes no change in the surface charge, thus minimizing possible effects on the photocycle kinetics. By using the procedure described in *Materials and Methods*, 0.65–0.95 mol of BMF per mol of bR was incorporated. In wild-type bR, which lacks cysteine, < 0.05 mol of BMF was bound under these conditions.

Absorption Spectrum and Photocycle. The wavelength maxima of the visible absorption spectra of the mutants were identical to that of wild type both before and after labeling. The photocycle kinetics were measured before and after derivatization. Fig. 2 shows the absorption changes at 410 nm due to the rise and decay of the M intermediate for wild type, G72C-MF, A160C-MF, and G231C-MF. The time constants and relative amplitudes describing the kinetics of M for these mutants as well as for V101C-MF and Q105C-MF are listed in Table 1. The three rise times of M are labeled τ_1 , τ_2 , and τ_3 . The kinetics were unaffected by the labeling. Fig. 2 shows that for G72C-MF, with the label on the extracellular side, the time trace coincides with that of wild type. For the other mutants with fluorescein on the cytoplasmic side, the kinetics were perturbed compared with wild type. For V101C-MF, Q105C-MF, and A160C-MF, only the decay of M was altered. For G231C-MF the rise of M was accelerated, and the decay contained an additional slow component (Fig. 2).

Proton Release Kinetics. The appearance of the proton at the surface and in the bulk was detected with the surface-bound fluorescein and the bulk indicator pyranine, respectively. With both dyes, all measurements were performed under the same conditions (22°C, pH 7.3, and 150 mM KCl). In Fig. 3 the kinetics of the rise and decay of the M intermediate are compared with the kinetics of proton release as detected by fluorescein and pyranine (DIFMF and DIFPY, respectively, in Fig. 3). Six exponentials are required to fit the time traces for M, the rise times being marked by the vertical arrows. The rise of the proton signals requires only one exponential, marked by a single arrow. The proton release time constants as detected by fluorescein and pyranine are listed in

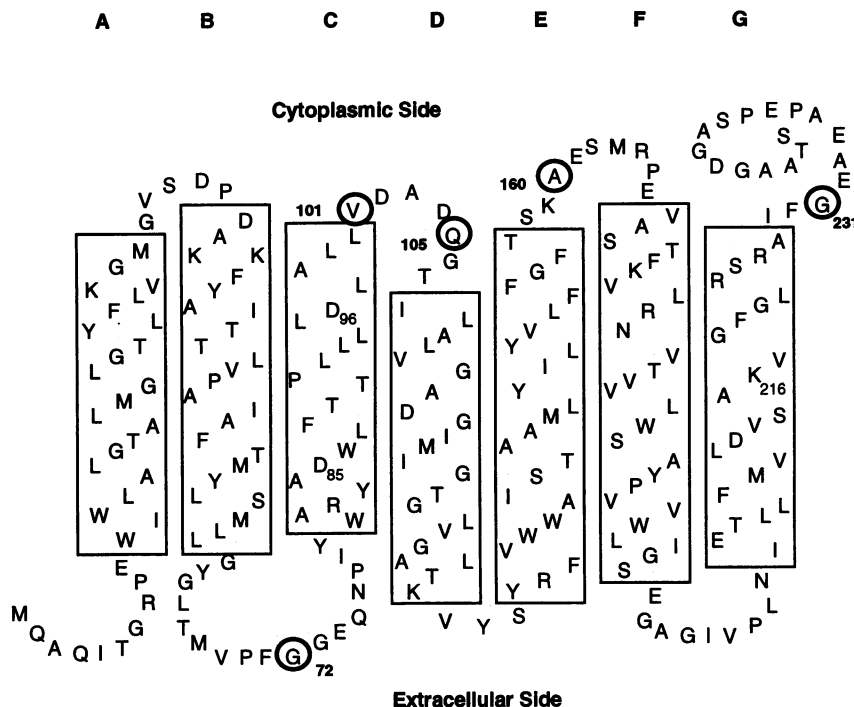


FIG. 1. Secondary structural model of bR. The residues changed to cysteine are indicated by circles.

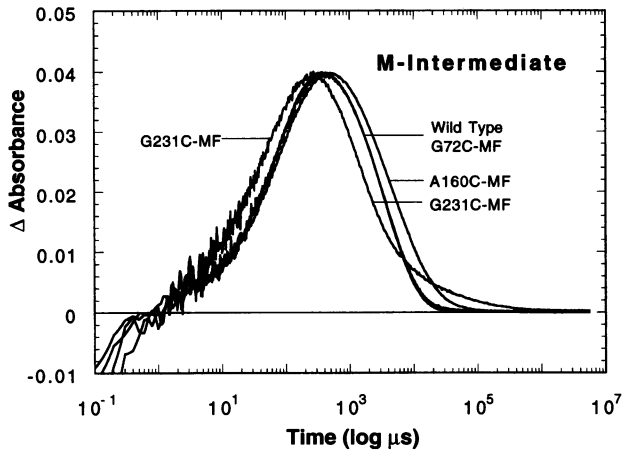


FIG. 2. Flash-induced absorbance changes at 410 nm for wild-type bR and the cysteine mutants G72C, A160C, and G231C after derivatization with fluorescein. Conditions: pH 7.3, 22°C, and 150 mM KCl. The logarithmic time scale is from 10⁻¹ to 10⁷ μs.

Table 1. Fig. 3A shows that the proton released on the extracellular side of the membrane was detected at the position G72C (i.e., on the same side) 71 μs after the flash, whereas pyranine detected the proton only after 850 μs. The proton release time of 71 μs falls between the two major rise times of M, τ₂ [45 μs (42%)] and τ₃ [152 μs (52%)]. For this mutant the photocycle kinetics were unperturbed (Fig. 2 and Table 1). Surprisingly, the results for proton detection with the dye bound on the opposite surface (the H⁺-uptake side) were quite similar (see Fig. 3B and C for A160C and G231C, and see Table 1 for V101C and Q105C). In all cases the proton was detected at the surface at least 10 times faster than in the bulk. As expected the bulk detection times were about the same for every mutant and close to the wild-type value (Table 1). In each case the proton-release time constant detected at the surface lay between τ₂ and τ₃ for the rise of M (Table 1). For V101C, Q105C, and A160C, the kinetics of the rise of M were virtually identical to each other and to that of wild-type, and the corresponding proton detection times were the same within experimental error: 77 μs (V101C), 76 μs (Q105C), and 74 μs (A160C). For G231C the rise of M is accelerated by a

Table 1. Time constants and amplitudes (%; in parentheses below the corresponding time) for the kinetics of the M intermediate and the proton release with fluorescein attached to various positions and with pyranine in the bulk phase

	H ⁺ release,		M rise, μs			bR sequence		
	μs					M decay, ms		
	FLU	PYR	τ ₁	τ ₂	τ ₃			
Wild type	—	820	2.2 (6)	49 (44)	147 (50)	2.2 (15)	3.4 (53)	6.8 (32)
Mutant								
Extracellular								
G72C-MF	71	850	1.1 (6)	45 (42)	152 (52)	2.4 (34)	4.0 (45)	9.0 (21)
Cytoplasmic								
V101C-MF	77	950	2.0 (7)	43 (58)	141 (35)	1.3 (67)	4.6 (31)	
Q105C-MF	76	920	1.0 (5)	50 (42)	160 (53)	2.4 (20)	6.6 (51)	17.7 (29)
A160C-MF	74	850	1.4 (5)	47 (41)	175 (54)	2.8 (44)	9.9 (52)	64.0 (4)
G231C-MF	60	820	1.4 (7)	24 (33)	101 (60)	2.2 (77)	11 (16)	130.0 (7)

Conditions were pH 7.3, 22°C, and 150 mM KCl. Flu and Pyr refer to the proton indicator dyes fluorescein and pyranine respectively.

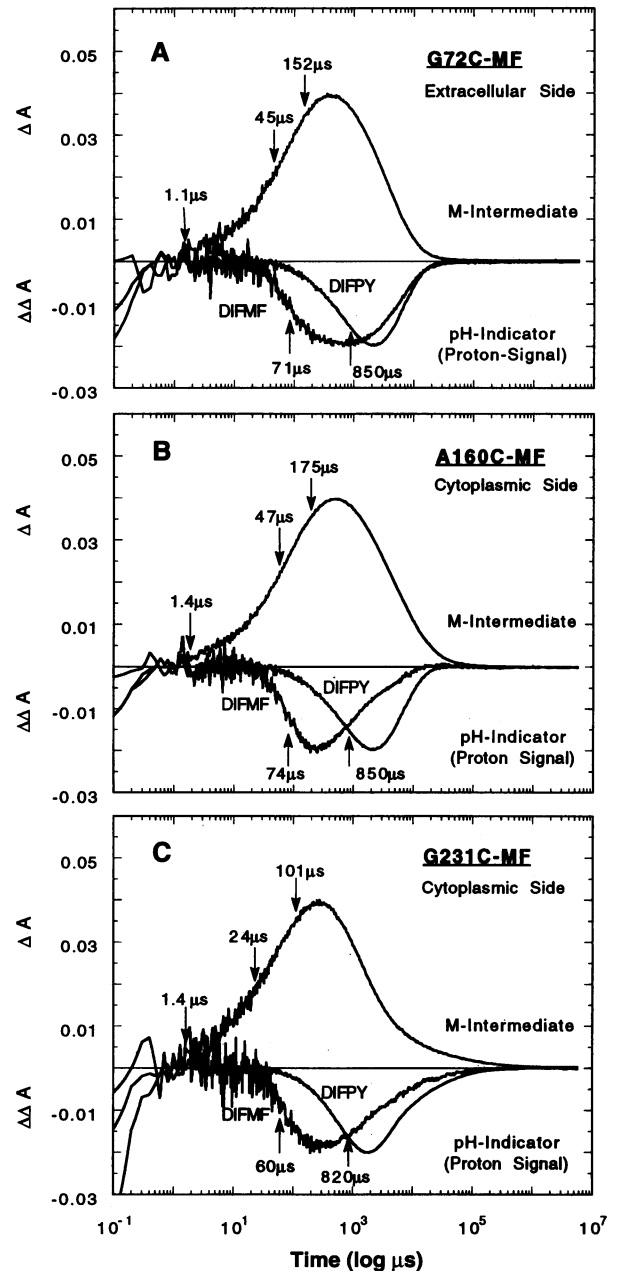


FIG. 3. Comparison of the rise and decay of the M intermediate with the kinetics of the proton release as detected with fluorescein bound on the extracellular side [G72C (A)] and on the cytoplasmic side [A160C (B) and G231C (C)] of the purple membrane. Conditions: pH 7.3, 22°C, and 150 mM KCl. The upper and lower parts of each panel contain the positive absorbance change ΔA at 410 nm due to M and the negative absorbance changes ΔΔA due to fluorescein at 495 nm (DIFMF) and to pyranine at 450 nm (DIFPY), respectively. The vertical arrows indicate the time constants obtained from a multiexponential fit. The fluorescein signal was scaled by a factor between 2 and 4 to give it the same amplitude as the pyranine signal.

factor of about 1.5. Interestingly, the corresponding proton detection time was also faster (60 μs), but the experimental error was considerable. When we compared the proton release times for the positions that have unaltered M-rise kinetics, we obtained for the extracellular side 71 ± 4 μs (G72C) and for the average value on the cytoplasmic side 76 ± 5 μs. The values for the two sides are thus virtually identical.

Temperature Dependence. To test for a kinetic correlation between the rise of M and the proton release, the rates were changed by varying the temperature between 5°C and 40°C for

G72C. The Arrhenius plots for τ_2 and τ_3 , the two major rise times of M, and the H^+ -release time are shown in Fig. 4. The plots are linear for τ_2 and τ_3 with almost equal activation energies of 68 ± 1 kJ/mol. For the proton release time, however, the Arrhenius plot is clearly nonlinear. It appears to have a break between 20°C and 25°C and seems to approach the straight line for τ_2 tangentially at low temperatures. The effective activation energy is clearly smaller. Thus, whereas at 5°C the proton release time equals τ_2 , at 40°C it is slower than the slowest component in the rise of M (τ_3).

DISCUSSION

The pathway of protons through bR consists of two parts: first the Schiff base proton is transferred to the extracellular surface, and subsequently the Schiff base is reprotonated from the cytoplasmic side of the membrane. Our observation that the proton release is detected 10 times faster on the cytoplasmic surface than in the bulk phase is evidence for the migration of protons along the purple membrane surface from the extracellular to the cytoplasmic side. Evidently, the protons appearing at the extracellular surface are initially trapped in the interfacial surface layer, with its negatively charged groups (8) and its high buffer capacity, and rapidly equilibrate along the surface. Transfer into the bulk occurs only with considerable delay. A schematic view of this interpretation is presented in Fig. 5. By rapid lateral proton diffusion, an equilibrium is established on both sides of the membrane within about 75 μ s, well before detection of protons in the bulk phase (880 μ s).

The present observations confirm and extend our previous results with monomeric bR micelles (5–7). In the micelle system we found proton release times of 57 and 60 μ s with fluorescein in positions 101 and 160 respectively, on the cytoplasmic side and of 125 μ s with pyranine in the bulk phase (5, 6). For purple membrane under the same experimental conditions, we now find proton release times of 77 and 74 μ s with fluorescein in the same positions and of 880 μ s with pyranine in the bulk phase. The difference between the proton detection times on the cytoplasmic side and in the bulk phase is thus much more pronounced for purple membranes than with the micelle system. The large difference in the proton detection times with pyranine in the two systems (125 versus

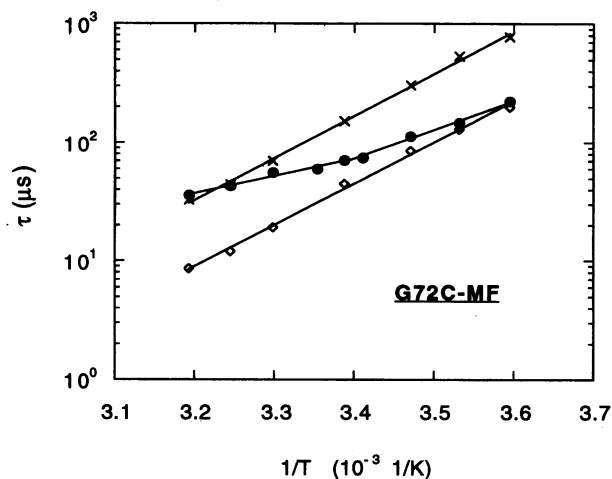


FIG. 4. Arrhenius plot of the time constants τ_2 (◇) and τ_3 (×) for the formation of the M intermediate and for the proton release (●) measured with fluorescein bound to position 72 (G72C-MF). The sample was at pH 7.3 in 150 mM KCl. From the slopes of the two linear plots for the rise of M, activation energies of 66.9 kJ/mol (◇) and 68.1 kJ/mol (×) were obtained. When the curved plot for the proton release was analyzed by assuming linear low- and high-temperature branches with a break around 22°C, the activation energies were 46.5 and 30.4 kJ/mol, respectively.

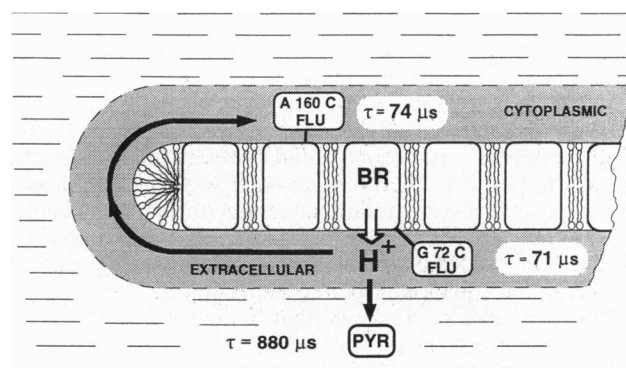


FIG. 5. Cartoon of proton flow along the surface and around the edge of a purple membrane patch and into the bulk. The figure is not to scale. The lateral dimension of the membrane is about 100 times larger than the thickness. The interfacial layer between membrane surface and bulk is marked in grey. The pH indicator dyes fluorescein and pyranine are indicated by FLU and PYR, respectively. Protons released on the extracellular side (bottom) are detected by covalently bound fluorescein on the cytoplasmic surface at position 160 well before they are detected by pyranine in the bulk (74 μ s after the flash versus 880 μ s). The proton release time on the extracellular surface at position 72 is 71 μ s. Arrows indicate schematically the lateral proton migration along the surface and the delayed transfer from the surface layer into the bulk. In the actual experiments, each bR molecule has one bound surface dye on one side only.

880 μ s) may be due to differences in buffer capacity, lipid headgroups, and surface charge. The purple membrane contains, for instance, a high percentage of anionic lipid headgroups such as phosphatidylglycerol phosphate. The fact that there is only a small difference in the proton detection times with fluorescein on the cytoplasmic side between purple membranes and the much smaller bR micelles suggests that the step around the purple membrane edge may be rate-limiting for the detection on the cytoplasmic side. Our finding that proton transfer into the bulk is much slower than proton diffusion along and around the purple membrane supports models of local proton coupling.

At 22°C the proton detection times on the two sides of the membrane are virtually identical, differing by at most a few microseconds (Table 1). What does this imply for the magnitude of the surface diffusion constant D (2, 14)? Assuming an average purple membrane radius of 0.25 μ m and a difference of less than 5 μ s between the proton detection times on the two sides, we find, using the relationship $\Delta r^2 = 4Dt$, that $D > 3 \times 10^{-5}$ cm²/s. More elaborate calculations should take into account the distribution of membrane sizes and diffusion distances. This rough estimate of D shows nevertheless that the surface diffusion is rapid and that it may even be larger than the diffusion constant of protons in bulk water (9×10^{-5} cm²/s).

Since deprotonation of the Schiff base is presumably a prerequisite for proton release, it is essential to verify that the kinetics of M formation are the same in all mutants and wild type. Otherwise, comparisons between proton detection times for the two surfaces become meaningless. We found that, except for G231C, the rise-time kinetics of M were unaffected by the mutations and the labeling. The decay kinetics of M were perturbed, however, in all of the cysteine mutants except G72C. No further changes were introduced by the fluorescein labeling. Mutations of residues in the cytoplasmic loops apparently lead to structural changes on that side of the membrane from which protons are taken up, thereby changing the kinetics of Schiff base reprotonation and of M decay. Similar changes were observed in the decay kinetics of M for the same mutants expressed in *Escherichia coli* and reconstituted in micelles (5, 6).

During the formation of the M intermediate, the Schiff base is deprotonated and the proton is transferred to Asp-85 (15). Whereas our data for G72C show that a proton is detected at the extracellular surface during the rise of M, about 71 μ s after the flash, it is generally believed that Asp-85 remains protonated for several milliseconds until the very last step of the photocycle (16, 17). Therefore, another group, XH, releases the proton, and possibly additional residues or water molecules are involved between Asp-85 and XH. Thus, there is no need for the rates of Schiff base deprotonation (M-rise) and of fluorescein protonation to be the same, and the temperature dependence of Fig. 4 shows that they do indeed differ. Nevertheless at 5°C the proton release time has the same value as the second rise time of M (τ_2), and its curved Arrhenius plot seems to approach the linear Arrhenius plot of τ_2 asymptotically at low temperatures. These observations suggest that at low temperatures the deprotonation of the Schiff base is rate limiting, whereas at higher temperatures a subsequent reaction step becomes rate limiting. If we model this with a sequential two-step unidirectional reaction scheme, this implies that the first reaction has the larger activation energy and that τ_2 should be identified with the deprotonation of the Schiff base. Contrary to our findings, a linear Arrhenius plot was obtained for the proton release time with fluorescein bound by chemical modification to Lys-129 on the extracellular surface (18). However, in agreement with our results, these authors found that at 10°C the proton release time equals the second rise time of M. Under almost the same conditions (pH 7.5, 22°C, and 150 mM KCl), they obtained a proton release time of $63 \pm 8 \mu$ s at position 129 equal within experimental error to our result of $71 \pm 4 \mu$ s at position 72.

The two-step model discussed above does not predict the existence of a second major component in the rise of M (τ_3). Currently, no satisfactory explanation for the occurrence of multiple times in the formation of M is available. It may be explained by (i) a M \rightarrow L backreaction in a cycle with a single M species, (ii) parallel cycles with different M rise times, and (iii) sequential M species in a single cycle. It was recently proposed that proton release is coupled to the transition between two sequential M species rather than to the L-to-M transition (19), and this possibility cannot be excluded from our experiments. Further progress has to await a definitive explanation for the multiple rise times of M. The data of Fig. 4 suggest, however, that τ_2 becomes rate limiting at low temperatures. The present experiments thus do not rule out the coupling between proton release and Schiff base deprotonation.

In conclusion, our data show that the protons released by bR on the extracellular side of the purple membrane are trapped at the surface and equilibrate so slowly with the bulk phase that

long-range lateral proton diffusion can occur along and around the purple membrane. These results support models of local movement of protons along energy-transducing membranes.

Note. After completion of this manuscript, we became aware of the article by Heberle *et al.* (20) describing partly similar experiments.

This research was supported by Grant GM28289 from National Institutes of Health (to H.G.K.), by Grant 03-HE3 FUB-6 from the Bundesministerium für Forschung und Technologie (to M.P.H.), and Grant Sfb 312/B1 from the Deutsche Forschungsgemeinschaft (to M.P.H.).

- Nagle, J. F. & Dilley, R. A. (1986) *J. Bioenerg. Biomembr.* **18**, 55–68.
- Teissie, J., Gabriel, B. & Prats, M. (1993) *Trends Biochem. Sci.* **18**, 243–246.
- Haines, T. H. (1983) *Proc. Natl. Acad. Sci. USA* **80**, 160–164.
- Gutman, M. & Nachliel, E. (1990) *Biochim. Biophys. Acta* **1015**, 391–414.
- Scherrer, P., Alexiev, U., Otto, H., Heyn, M. P., Marti, T. & Khorana, H. G. (1992) in *Structures and Function of Retinal Proteins*, ed. Rigaud, J. L. (Libbey, London), Vol. 221, pp. 205–211.
- Scherrer, P., Alexiev, U., Marti, T., Khorana, H. G. & Heyn, M. P. (1994) *Biochemistry* **33**, 13684–13692.
- Alexiev, U., Marti, T., Heyn, M. P., Khorana, H. G. & Scherrer, P. (1994) *Biochemistry* **33**, 13693–13699.
- Alexiev, U., Marti, T., Heyn, M. P., Khorana, H. G. & Scherrer, P. (1994) *Biochemistry* **33**, 298–306.
- Steinhoff, H.-J., Mollaaghababa, R., Altenbach, C., Hideg, K., Krebs, M. P., Khorana, H. G. & Hubbell, W. L. (1994) *Science* **266**, 105–107.
- Krebs, M. P., Mollaaghababa, R. & Khorana, H. G. (1993) *Proc. Natl. Acad. Sci. USA* **90**, 1987–1991.
- Otto, H., Marti, T., Holz, M., Mogi, T., Lindau, M., Khorana, H. G. & Heyn, M. P. (1989) *Proc. Natl. Acad. Sci. USA* **86**, 9228–9232.
- Kano, K. & Fendler, J. H. (1978) *Biochim. Biophys. Acta* **509**, 289–299.
- Fothergill, J. E. (1964) in *Fluorescent Protein Tracing*, ed. Nairn, R. C. (Livingstone, Edinburgh), pp. 34–59.
- Polle, A. & Junge, W. (1989) *Biophys. J.* **56**, 27–31.
- Braiman, M. S., Mogi, T., Marti, T., Stern, L. J., Khorana, H. G. & Rothschild, K. J. (1988) *Biochemistry* **27**, 8516–8520.
- Müller, K. H., Butt, H. J., Bamberg, E., Fendler, K., Hess, B., Siebert, F. & Engelhard, M. (1991) *Eur. Biophys. J.* **19**, 241–251.
- Bousché, O., Sonar, S., Krebs, M. P., Khorana, H. G. & Rothschild, K. J. (1992) *Photochem. Photobiol.* **56**, 1085–1095.
- Heberle, J. & Dencher, N. A. (1992) *Proc. Natl. Acad. Sci. USA* **89**, 5996–6000.
- Zimanyi, L., Váró, G., Chang, M., Ni, B., Needleman, R. & Lanyi, J. K. (1992) *Biochemistry* **31**, 8535–8543.
- Heberle, J., Riesle, J., Thiedemann, G., Oesterhelt, D. & Dencher, N. A. (1994) *Nature (London)* **370**, 379–382.